

FACTA UNIVERSITATIS

Series: **Electronics and Energetics** Vol. 30, N° 3, September 2017, pp. 267 - 284

DOI: 10.2298/FUEE1703267A

RECENT ADVANCES IN NTC THICK FILM THERMISTOR PROPERTIES AND APPLICATIONS

Obrad S. Aleksić¹, Pantelija M. Nikolić²

¹Institute for Multidisciplinary Research, University of Belgrade, Serbia

²Serbian Academy of Sciences and Arts, Belgrade, Serbia

Abstract. *An introduction to thermal sensors and thermistor materials is given in brief. After that novel electrical components such as thick film thermistors and thermal sensors based on them are described: Custom designed NTC thermistor pastes based on nickel manganite NiM_2O_4 micro/nanostructured powder were composed and new planar cell-based (segmented) constructions were printed on alumina. The thick film segmented thermistors were used in novel thermal sensors such as anemometers, water flow meters, gradient temperature sensor of the ground, and other applications. The advances achieved are the consequence of previous improvements of thermistor material based on nickel manganite and modified nickel manganite such as $\text{Cu}_{0.2}\text{Ni}_{0.5}\text{Zn}_{1.0}\text{Mn}_{1.3}\text{O}_4$ and optimization of thick film thermistor geometries for sensor applications. The thermistor powders were produced by a solid state reaction of MnCO_3 , NiO , CuO , ZnO powders mixed in proper weight ratio. After calcination the obtained thermistor materials were milled in planetary ball mills, agate mills and finally sieved by 400 mesh sieve. The powders were characterized by XRD and SEM. The new thick film pastes were composed of the powders achieved, an organic vehicle and glass frit. The pastes were printed on alumina, dried and sintered and characterized again by XRD, SEM and electrical measurements. Different thick film thermistor constructions such as rectangular, sandwich, interdigitated and segmented were printed of new thermistor pastes. Their properties such as electrical resistance of the thermistor samples were mutually compared. The electrode effect was measured for all mentioned constructions and surface resistance was determined. It was used for modeling and realizations of high, medium and low ohmic thermistors with different power dissipation and heat loss. Finally all the results obtained lead to thermal sensors based on heat loss for measuring the air flow, water flow, temperature gradient and heat transfer from the air to the ground.*

Key words: *Metal oxide thermistors, thick film thermistor geometries, thick film thermistor sensors and systems*

Received November 10, 2016

Corresponding author: Obrad S. Aleksić

Institute for Multidisciplinary Research, University of Belgrade, Kneza Višeslava 1a, 11 000 Belgrade, Serbia
(E-mail: obradal@yahoo.com)

1. INTRODUCTION TO TEMPERATURE SENSORS

Temperature measuring and control today is widely spread everywhere around us: from homes and buildings, ground surface, water and air to power machines in industry, cars and trucks, electronic equipments, chemistry, medicine etc. [1-4]. The temperature measuring range is divided in several sub-ranges such as cryogenic -temperatures, near-room temperatures, moderate elevated temperatures, and high temperatures. To cover these temperature ranges with measuring different temperature measuring methods and temperature sensor devices were developed mainly based on thermocouples (thermoelectric effect), thermistors (thermo resistive effect) and pyrometers (infrared to visible light radiation) [5-7].

The thermoelectric effect was discovered by Seebeck in 1821. The thermocouple was formed of two wires of different metals joined in one point by welding [8]. The thermoelectric electromotive force - EMF depends on metals used in forming the thermocouple. There are various combinations of metals such as copper and iron, metal alloys of Alumel (Ni/Mn / Al/Si), Chromel (Ni/Cr), Constantan (Cu/Ni), Nicrosil (Ni/ Cr/Si) and Nisil (Ni/ Si/Mn), the noble metals platinum and tungsten, and the noble-metal alloys of platinum/rhodium and tungsten/rhenium [9]. The output of thermocouples increases with temperature increase from low temperatures to moderate and high temperatures. The platinum rhodium-platinum thermocouple reaches 20 mV at 1600 °C, chromel-alumel 50 mV at 1200 °C and chromel-constantan 80 mV at 1000° C, while at cryogenic temperatures round 0 K voltage EMF is negative and reaches -6 mV for copper-constantan and -10 mV for chromel-AuFe wires. EMF of thermocouples is non-linear function of temperature t [°C] which crosses zero at 0 °C. It can be approximated by following equation: $e = a_1t + a_2t^2 + a_3t^3 + a_4t^4 \dots$ where $a_1, a_2, a_3, a_4 \dots$ are constants experimentally determined. Inaccuracy is round $\pm 0.2\%$ of the EMF voltage or ± 2 °C at 1000 °C, for example [10].

At higher temperatures optical pyrometers are used for measuring temperatures using Stefan–Boltzmann law [11]. The output signal of the photo detector is related to the thermal radiation or irradiance $j^* = \varepsilon \sigma T^4$, where σ is called the Stefan-Boltzmann constant and ε is the emissivity of the object. The temperature T is measured from the distance (1-10 meters) and the measuring temperature range of pyrometers is typically from 650-2500 °C. The pyrometer inaccuracy is high, typically round $\pm 25^\circ$ C at the beginning of the measuring range and ± 50 °C at the end of the measuring range [12].

Thermistors are a new class of temperature sensors based on the thermo-resistive effect [13,14]. It includes sintered metal oxides (electronic ceramics) exhibiting different values of resistance thermal coefficients in near-room and moderate temperature range. Generally their resistance temperature coefficient can be positive or negative (PTC and NTC, respectively). PTC thermistors are used in heaters, temperature level controls and thermal switches while NTC thermistors are used in temperature measurements in electronic equipment, air conditioning, cars, domestic appliances etc. [15]. The main advantage of this class of sensors compared to thermocouples is small dimensions, high sensitivity and low price: thermistors are mass produced as electronic components with one pair of leads (small disc shape), or with short leads (small cubic chips) like other SMD components (figure1) [16]. The nominal resistance for example is in the range from $1k\Omega$ to 10k, temperature application range from -50 to 150 °C and sensitivity is 3-5 % per °C, which is much higher compared to thermocouples. The resistance temperature coefficient

values round $B=4000$, for example and resistance R decreases with temperature T increase by exponential law such as: $R = R_0 \exp [B*(1/T - 1/T_0)]$, R_0 -nominal thermistor resistance measured at $T_0= 293$ K (20° C). It enables easy temperature measurement with inaccuracy of $\pm 0.1^\circ$ C or less [17]. It also can be used for surge protection, delay in electronic circuits and temperature compensation in power electronic circuits. Therefore there is a permanent interest in thermistor materials innovation and development for new applications.

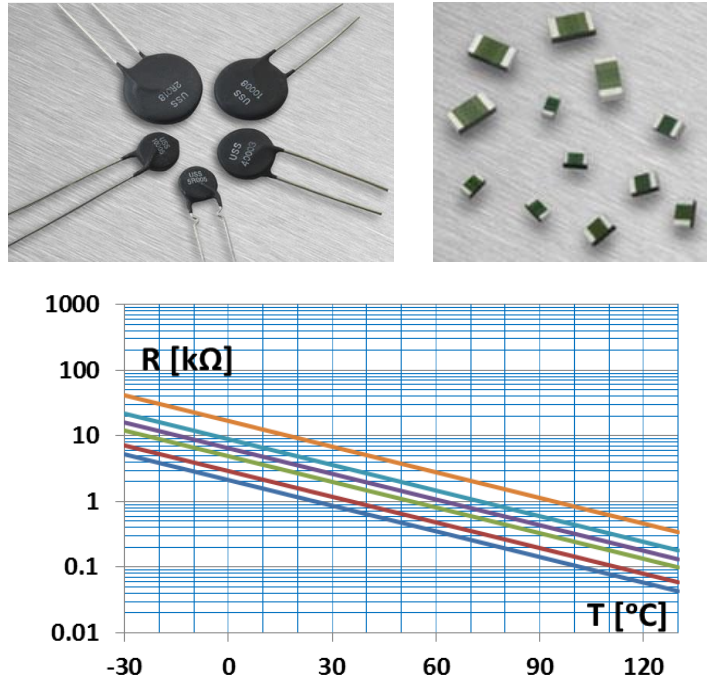


Fig. 1 Disc and chip thermistors based on sintered metal oxides (top figures): leaded and leadless- left and right respectively, and typical resistance values R vs. temperature T for commercial nickel manganese NTC thermistors (bottom).

Comparison of typical values of the main characteristics of NTC thermistors, Platinum resistors (RTD), thermocouples and semiconductor thermal sensors from the application aspect is given in table 1 [18-20].

One of the way to reach new thermistor applications is use of thick films custom design thermistor pastes (modified micro/nano structure, partly substitution of metals, even doping with Re) and new planar constructions adapted by shape and size to required resistance and power. The objectives are measuring of moderate elevated temperatures, flow of gasses and liquids by heat loss thermistors (flowmeters), measuring of heat transfer through the surface or heat radiation (bolometers), temperature gradient in the ground, water and air.

Table 1 Comparison of modern temperature sensor devices

	NTC Thermistor	Platinum RTD	Thermocouple	Semiconductor
Sensor	Ceramic (metaloxide spinel)	Platinum wire or metal film	Thermoelectric	Semiconductor Junction
Temperature range	-100 to +325°C	-200 to +650°C	-200 to +1750°C	70 to 150°C
Accuracy	0.05 to 1.5°C	0.1 to 1.0°C	0.5 to 5.0°C	0.5 to 5.0°C
Stability at 100°C	0.2°C/year (epoxy) 0.02°C/year (glass)	0.05°C/year (film) 0.002°C/year (wire)	Variable, some types very prone to aging	>1°C/year
Output	NTC Resistance -4.4%/°C typical	PTC resistance 0.00385Ω/Ω/°C	Thermovoltage 10μV to 40μV/°C	Digital, various Outputs
Linearity	Exponential	Fairly linear	Most types nonlinear	Linear
Response time	Fast 0.12 to 10 s	Slow 1 to 50 s	Fast 0.10 to 10 s	Slow 5 to 50 s
Cost	Low to moderate	Wire - High Film - Low	Low	Moderate

Thick film technology enables miniaturization of thermistors, faster thermistor response, mass production, integration with electronics and realizing novel geometries such as row and matrix of thermistors, segmented geometry, multilayer and interdigitated geometry. They can be modified in shape to cover the heat source or measuring requirements for differential measurement (in defined point) or average measurements (on defined surface).

This work deals with recent research on thermistor materials and their applications: from powder preparation, pressed and sintered samples, thick film pastes to thick films devices, including our contributions to that field in last two decades. Our intention was to govern thermistor properties by finding out correlations between their electronic properties and micro/nano structure and between thick film geometry and electrical properties, to optimize the sensitivity, reliability, reproducibility, robustness, long term stability etc., and answer the specific requirements in new sensor applications as mentioned above. The authors expect new sensor products in the market based on thick film thermistors in the near future.

2. METAL OXIDE THERMISTORS

Thermistors were invented in 1930 and their name is a combination of the words thermal and resistor: THERMal-resISTORS [22]. The first thermistors were made of metal oxide powders mixture pressed and sintered at elevated temperatures. Generally, they are classified into two types: (PTC) thermistors where resistance increases with increasing temperature, and the device is called a positive temperature coefficient thermistor, and (NTC) thermistor where the resistance decreases with increasing temperature, and the device is called a negative temperature coefficient thermistor. Moreover they are also classified in two groups such as thermistors for low temperature operation (-50 to 150°C) and high temperature operation (150 to 900°C) [23,24].

A large number of metal oxides have decrease of resistance with temperature increase, and their sign is defined as NTC, but they are not used as thermistor materials if their electrical resistance is too high. The most suitable values of thermistor resistances for temperature measurement and control in electronics or as temperature sensors at room temperatures are moderate values (from 1-10 kΩ). The materials that can be used in synthesis

of thermistors for low temperature range of -50 to 150 °C are mixed oxides of Mn, Ni, Co. They have a spinel structure such as: $(\text{NiMn})_3\text{O}_4$, $(\text{NiMnCo})_3\text{O}_4$, $(\text{NiMnFeCo})_3\text{O}_4$ or cubic structure like $(\text{Fe,Ti})_2\text{O}_3$ and can be doped with other metal oxides such as LiO, RuO_2 , ZnO, CuO, CoO etc. [25,26]. Their bulk resistance ρ_{25} of powder pressed and sintered samples which are measured at room temperature is correlated with exponential coefficient B of bulk resistance and compared (figure 2)[27]. The small addition of Co in spinel gives higher B values and higher values of resistance [28-30]. The resistance is the consequence of initial powder properties, sintering temperatures/time profiles and microstructure of the samples [30-36].

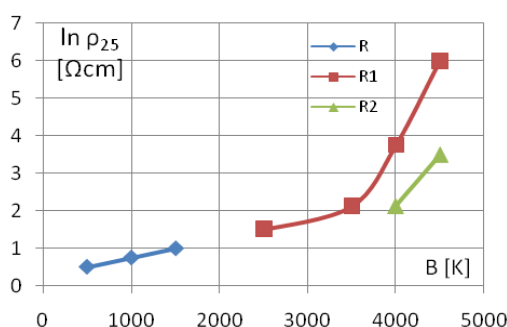


Fig. 2 Corellation between bulk resistivity and exponential coefficient of resistivity B for different NTC thermistor materials: curve R – (Mn, Ni, Co), Li – doped ; curve R1 – spinel group $(\text{NiMn})_3\text{O}_4$, $(\text{NiMnCo})_3\text{O}_4$, $(\text{NiMnFeCo})_3\text{O}_4$; curve R2 – $(\text{Fe,Ti})_2\text{O}_3$.

The materials that can be used in synthesis of thermistors for high temperature range of 150 to 1100 °C are mixed oxides such as $\text{Mg}(\text{Al}_{1-x}\text{Cr}_x)_2\text{O}_4$ [37], Y-Al-Mn-Fe-Ni-Cr-O [38], $\text{MgAl}_2\text{O}_4\text{-LaCr}_{0.5}\text{Mn}_{0.5}\text{O}_3$ [39], CaTiO_3 [40], $\text{Sr}_7\text{Mn}_4\text{O}_{15}$ [41], $\text{Ni}_{1.0}\text{Mn}_{2-x}\text{Zr}_x\text{O}_4$ [42], Fe_2TiO_5 [43], BaTiO_3 [44], $\text{Al}_2\text{O}_3\text{-Cr}_2\text{O}_3\text{-ZrO}_2$ [45] etc. Their properties such as temperature operating range, resistance and exponential factor B are given in table 2.

Table 2 High temperature NTC thermistor materials

	Operating range [°C]	T [°C]	Resistivity [$\Omega\cdot\text{cm}$] at T	B [K]
$\text{La}_2\text{O}_3\text{-Al}_2\text{O}_3\text{/Cr}_2\text{O}_3, \text{CuO}$	50-600	50, 600	$3\cdot 10^{11}, 5\cdot 10^4$	10^4
$\text{Bi}_2\text{Zr}_3\text{O}_7$	250-600			$11\text{-}17\cdot 10^4$
$\text{ZrO}_2\text{/CaO}$	400-1000	400, 1000	$5\text{-}6\cdot 10^5, 20$	
$\text{CoO-TiO}_2\text{/Cr}_2\text{O}_3$	620-1100			$22,8\cdot 10^3$
$\text{CoO-TiO}_2\text{/Y}_2\text{O}_3$	620-1100			$31,1\cdot 10^3$
$\text{TiO}_2\text{-CoO/Y}_2\text{O}_3$	650-1100			$28\cdot 10^3$
$\text{MnO-Al}_2\text{O}_3\text{-Na}_2\text{O 1:2:4.8}$	20-600	20	$9\cdot 10^8$	$14,4\cdot 10^3$
$\text{CeO}_2\text{/PrO}_2$	200-1200			$10\text{-}15\cdot 10^3$

The high temperature thermistors are usually disc and chip type, sealed in glass with Pt wire terminations. The ceramic type special glass have a strength more than two times that of traditional glass-coated products and have excellent durability against reducible

gases, such as hydrogen gas. Their accuracy is lower than the low temperature thermistors like nickel manganese thermistors NiMn_2O_4 . Therefore they are used in applications that directly detect high temperatures in regions to be heated: burner temperature control in gas ranges and soldering tool, oil heaters, for other abnormal heating detection in combustion equipment, and for industrial equipment instead platinum temperature detectors and thermocouples.

3. THICK FILM THERMISTOR PASTES

Thick film pastes are composed of the fine powders of thermistor materials, organic vehicle and glass frits as a binder to ceramic substrate. The most often used thermistor pastes are based on nickel-manganese NiMn_2O_4 where nickel is substituted partly with Co [46,47] and nickel manganese is substituted with Zn, Cu [48-50]. The base material nickel manganese can be doped with Bi, La, Sn, Cr, Ru, Al oxides to improve stability of electrical characteristics in the temperature operation range and adjust exponential factor B [50-55]. Moreover our contribution to thick film thermistor layers includes not only substitution of basic oxides with other oxides but development of pastes based on thermistor nanopowders [56]. The sintered thermistors electronic properties were measured by FIR spectrometers [57,58], Hall effect measurement [59], electrical measurement (activation energy) [60] and photoacoustic spectroscopy (PA). The thermistor material thermal diffusivity was also determined for the first time by PA [61-63]. XRD of thermistor powders and SEM of recently developed low resistance thick film thermistors layers based on NiMn_2O_4 partly substituted with CuO and ZnO are given below in figures 2 and 3. The NTC behavior of the thick films is given in figure 4, while electronic properties are given in table 4 [64].

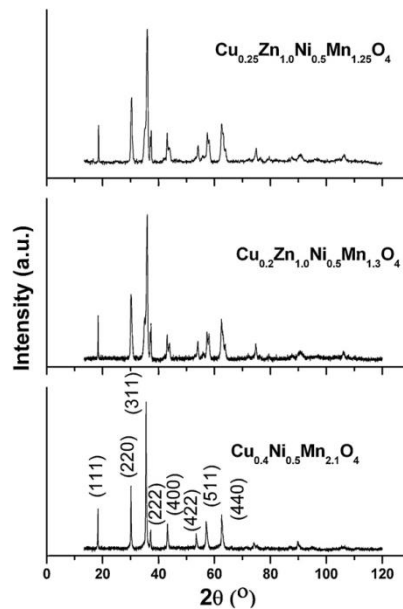


Fig 2 XRD of thermistor powder based on modified nickel manganese NiMn_2O_4 (substituted partly with ZnO and CuO) and used for thermistor pastes preparation.

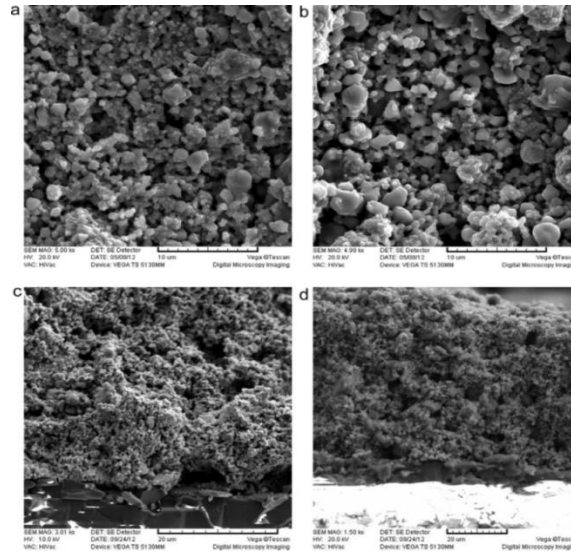


Fig. 3 SEM of NTC thick film thermistor layers sintered in the air at $850^\circ\text{C} / 10$ min: $\text{Cu}_{0.25}\text{Ni}_{0.5}\text{Zn}_{1.0}\text{Mn}_{1.25}\text{O}_4$ and $\text{Cu}_{0.4}\text{Ni}_{0.5}\text{Mn}_{2.1}\text{O}_4$: (a and b) sample surfaces, respectively and (c and d) sample cross sections, respectively.

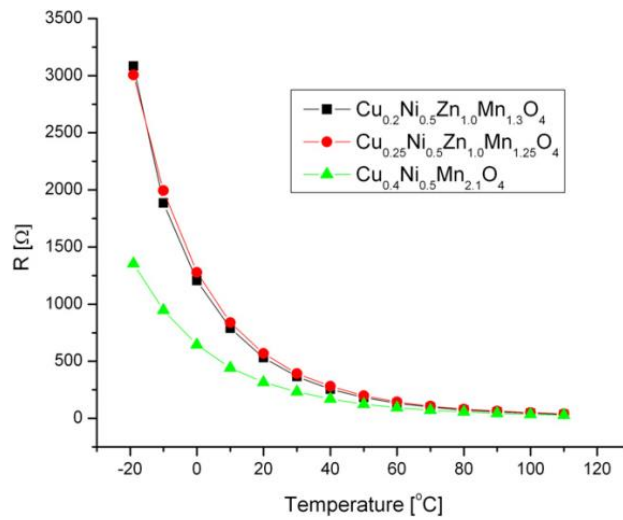


Fig. 4 NTC behavior of micro/nanostructured thick film thermistors based on NiMn_2O_4 partly substituted with CuO and ZnO .

Table 3 Electronic properties of NTC thermistor nanostructured thick films

Thermistor composition	R_{sq} [$M\Omega/sq$]	B [K]	E_a [eV]
$Cu_{0.2}Ni_{0.5}Zn_{1.0}Mn_{1.3}O_4$	1.3	3356	0.294
$Cu_{0.25}Ni_{0.5}Zn_{1.0}Mn_{1.25}O_4$	1.2	3294	0.288
$Cu_{0.4}Ni_{0.5}Mn_{2.1}O_4$	0.39	2915	0.255

The electrical surface resistance R_{sq} (sheet resistance) of thick film thermistors was measured on rectangular resistor geometry 2.5×2.5 mm printed on PdAg electrode matrix. Thick films printed of pure $NiMn_2O_4$ thermistor paste composed of round 0.9 micron powder has more than 10 times higher electrical resistance. The resistances were measured at room temperature (20 °C). The exponential factor B of thick film thermistor was determined from resistances R_{20} and R_{30} measured at 20 and 30 °C in the climatic chamber. Activation energy E_a is defined as $E_a = B \cdot k$, where k is Boltzmann constant.

4. THICK FILM THERMISTOR GEOMETRIES

Thermistor resistance R is complex function of sheet resistivity, geometry (shape and size), temperature T, and time t. The sheet resistance $\rho(k)$ changes with k inter-electrode spacing due to electrode effect e.g. the diffusion of conductor layer to the thermistor layer. Far enough from electrodes (k=few mm) practically there is no diffusion of metal electrodes to resistive layer at sintering temperature of 850 °C/10 min and sheet resistance is constant and marked with ρ_{bulk} . But this is not nominal resistance of the thermistor paste: it is conventional to use rectangular resistor geometry 2.5×2.5 mm (Du Pont test resistor) to determine nominal resistance of the pastes, together with electrode effect. In fact during printing the other un-homogeneity in layer deposition occurs (thickness deformations) that can vary the resistance along the resistor [65]. The ideal resistor R is dependent of resistor length-l, width-w, thickness -d, and number of layers-n) and it can be easily calculated. The NTC behavior has an exponential factor $A \cdot \exp(-B/T)$ where B is exponential temperature coefficient, A is constant. Moreover, thermistor resistance is dependant of time f(t): it is increasing lineal function (few seconds) and when heating is higher than cooling NTC effect occurs and further resistance it is decreasing function of time. Finally the equation which describes thermistor resistance is given as follows:

$$R = \rho(k)R(l, w, d, n)Ae^{-\frac{B}{T}}f(t) \quad (1)$$

The most difficult for modeling is f(t) as the heat transfer from thick film thermistor to air depends of shape and size of thermistor which can be different depending of application. The rectangular thermistors measure temperature in the defined point, while the surface planar thermistor constructions can measure temperature radiation flux, or average temperature of the surface, heat loss in fluids etc. For example different planar thick film thermistor constructions such as rectangular, sandwich, multilayer, segmented and interdigitated are given in figure 5. Their ideal resistance is modeled as R(l, w, d, n) and sheet resistance as $\rho(k)$, k-electrode spacing [66].

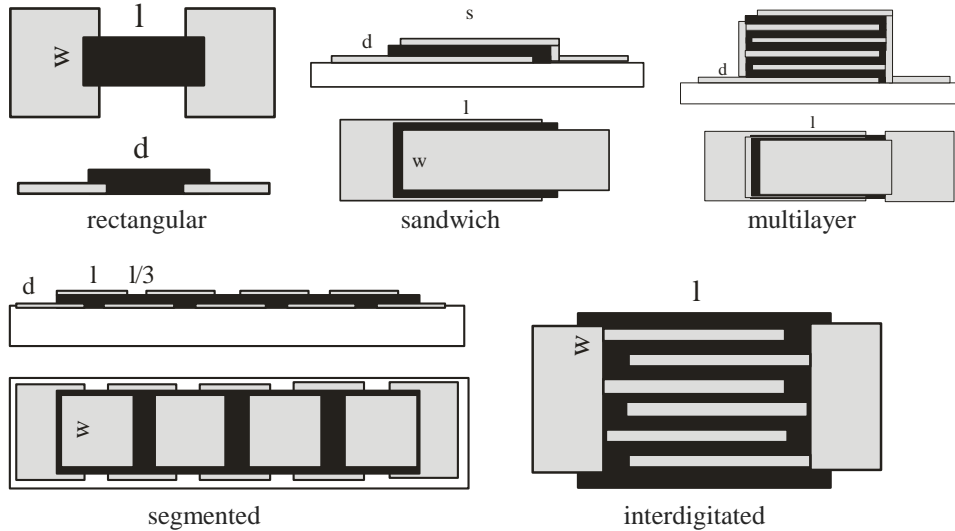


Fig. 5 Different thick film thermistor constructions (top view and cross section); rectangular, sandwich, multilayer, segmented and interdigitated, respectively. Gray area – PdAg conductive paste, black – NTC thermistor layer.

The sheet resistance $\rho(k)$ changes with k inter-electrode spacing as given in figure 6. The highest electrode effect which affects sheet resistivity $\rho(k)$ occurs in sandwich, multilayer and segmented constructions. The electrode spacing in that case is only 30-33 microns (three sequentially printed and fired thermistor layers), while in case of rectangular and interdigitated construction spacing is 1 mm or more. Sheet resistivity $\rho=20-32$ [Ωm] for low k and $\rho=275-285$ [Ωm] for $k>1$ mm respectively.

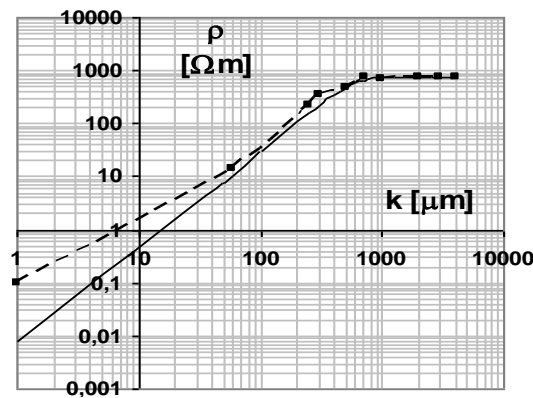


Fig. 6 The sheet resistivity ρ of thick film thermistors versus inter-electrode spacing k . Dashed line are experimental data measured at room temperature and solid line is modeled (fitted) $\rho(k)$ – determined by an exponential function.

The simple modeling of sheet resistance is done using following equation:

$$\rho(k) = \rho_{bulk} (1 - e^{-(k/k_0)^2}) \quad (2)$$

where $k=0$, $\rho=0$; $k \gg k_0$, $\rho = \rho_{bulk}$; $k=k_0=1\text{mm}$, $\rho = \rho_{bulk}(1-1/e)$. The model data differ from the experimental data (figure 6) for thermistor layer thickness less than 30 microns: sheet resistivity never crosses zero value as the diffusion of conductor PdAg to NTC thermistor layer is limited by finite porosity of thermistor microstructure (electrode effect saturation).

Thick film segmented thermistor is a novel construction developed for heat loss sensor applications as it has gradient of temperature along the fluid flow. Its electrical equivalent scheme consists of serial and parallel resistances R_s and R_p and serial and parallel capacitances C_s and C_p arranged between bottom and top electrodes and between the neighbour electrodes in the same row of electrodes (figure 7). Different thick film segmented thermistors are given in figure 8.

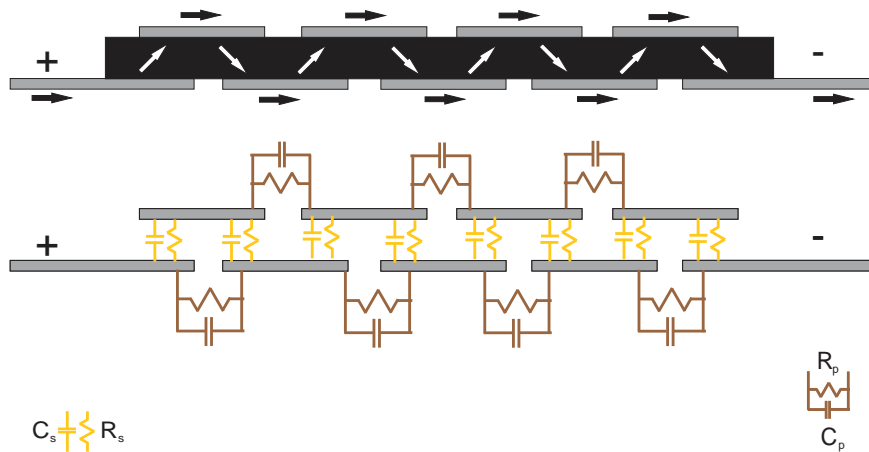


Fig. 7 Equivalent electrical scheme of segmented thick film thermistor construction:

R_s – serial resistor, C_s – serial capacitance, R_p – parallel resistor, C_p – parallel capacitor.

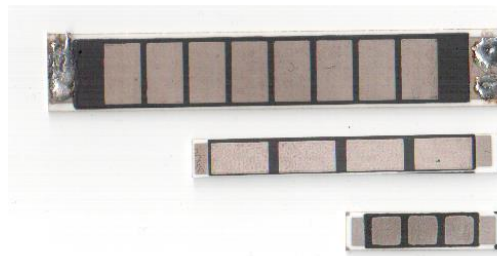


Fig. 8 Different thick film segmented thermistors: 5W (76.7 × 12.7 mm), 2W (51 × 6.35 mm) printed of NiMn_2O_4 paste and 1W (25.4 × 6.35 mm) printed of modified paste $\text{Cu}_{0.25}\text{Ni}_{0.5}\text{Zn}_{1.0}\text{Mn}_{1.25}\text{O}_4$.

Total resistance R of thick film segmented thermistor in DC regime is given with $R=2n \cdot R_s = \rho \cdot 2n \cdot d / ((l/3) \cdot w)$ (w – electrode width, l –electrode length, $l/3$ electrode spacing, n – number of top electrodes as given in figure 5), parallel resistors $R_p \gg R_s$ is neglected. In DC regime only resistances are active and in AC regime both resistances and capacitances are active and forms low band pass filter [67, 68]. In the segmented thermistor construction $R_p \gg R_s$ and $C_s \gg C_p$. The voltage applied on segmented thermistor is distributed over segments (cells) in accordance with R_s value.

5. THICK FILM THERMISTOR SENSORS AND SYSTEMS

Thermistor temperature sensors generate output signals in one of two ways: 1. through a change in output voltage (constant current) 2. through a change in resistance of the sensor's electrical circuit. Sensing methods: contact and non-contact. The contact method: sensor is in direct physical contact with the object to be sensed to monitor solids, liquids, gases over wide range. The non-contact method interprets the radiant energy of a heat source to energy in electromagnetic spectrum monitor non-reflective solids and liquids (thermistor bolometers). Temperature is a scalar quantity that determines the direction of heat flow between two bodies.

Temperature measuring and control by thermistors is enabled using Steinhart-Hart equation [69].

$$R(t) = A \exp\left(\frac{B}{T} + \frac{C}{T^2} + \frac{D}{T^3}\right) \text{ or } \frac{1}{T} = A + B(\ln R) + C(\ln R)^3 \quad (3)$$

A, B, C are constants determined experimentally. In the first approximation two thermistor resistances R_0 at $T_0 = 293,16$ K and R_1 at temperature T_1 are connected with following equation:

$$R_1 = R_0 \exp\left[\frac{B(T_0 - T)}{TT_0}\right] \text{ or } T_1 = \left[\left(B \cdot T_0 / (B + T_0 \ln \frac{R_1}{R_0})\right)\right] \quad (4)$$

Unknown temperature T_1 is defined by measuring R_1 and using ratio R_1/R_0 (4). The methods for calibration and linearization of NTC thermistors for high precision temperature measurements are given in literature [70-72]. The temperature gradient (in the air, water or ground) can be measured by segmented thick film thermistors using inner electrodes (see figure 7): for measured resistances R_1, R_2, R_3 and R_4 on segments, for example, temperatures T_1, T_2, T_3 and T_4 are determined using equation (4), respectively.

The first application of segmented thermistor as heat loss sensor was attempted in air flow measuring e.g. in anemometers [73-76]. After that three dimensional anemometer comprising thick film segmented thermistors, was formed using three uniaxial anemometers positioned under compasses to measure wind velocity as a three dimensional vector having $\{x, y, z\}$ projections on X,Y,Z axes, respectively. The module of wind vector velocity $|v|$ was calculated from square root of projections as $|v| = (x^2 + y^2 + z^2)^{1/2}$ and angles of wind vector to axes were calculated by from $\arctg \{(x/v), (y/v), (z/v)\}$. Three dimensional anemometer construction is given in figure 9, while the response of uniaxial anemometer I_{th} of selfheated thermistor on wind velocity change (v) is given in figure 10 for room temperature of the air.

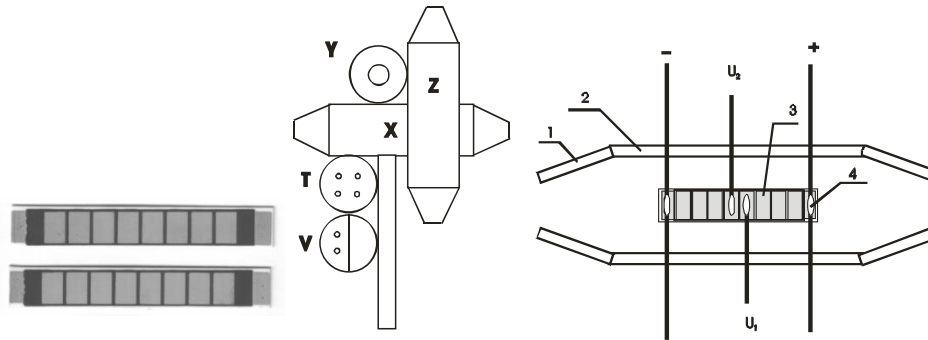


Fig 9 Three dimensional anemometer comprising thick film segmented thermistors: Thick film segmented thermistors - top view (right); Anemometer construction (figure in middle): X,Y,Z - three uniaxial anemometers positioned under compasses, T – input air thermometer, V – humidity sensor with thermistors; cross section of uniaxial anemometer (right): (+, -) power supply, U_1, U_2 inner electrodes, 1 – air flow reductor, 2 – sensor housing (tube), 3 – segmented thermistor.

The segmented thermistor is selfheated at constant voltage, and wind blow causes a heat loss on it's surface e.g., causes change of self resistance (increase), which further causes decrease (lowering) of selfheating current. The wind direction in uniaxial anemometers is determined by gradient of voltages using voltage difference ($U_1 - U_2$) on inner electrodes for two halves of selfheating segmented thermistor (figure 9 - right).

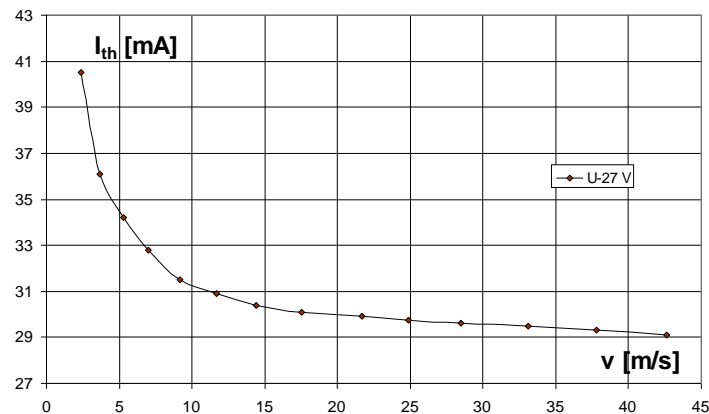


Fig. 10 The selfheating current I_{th} of segmented thermistor in uniaxial anemometer as response on input air velocity v (measured at room temperatures in aerodynamic tunnel).

The heat loss volume water flow sensor (flowmeter for water) was formed with two segmented thermistors as micro flowmeter and flowmeter for stationary flow [77-78]. The water flowmeter for unstationary flow aimed for waterworks current volume flow measuring was formed of segmented thermistors with reduced dimensions printed on

alumina of $\text{Cu}_{0.25}\text{Ni}_{0.5}\text{Zn}_{1.0}\text{Mn}_{1.25}\text{O}_4$ thermistor paste (figure 11). It consists also of two segmented thermistors: the first segmented thermistor (R) measures the input water temperature using $R(T)$ using equation (4) and the second is selfheated thermistor at constant voltage (U). The selfheated current I is changed with water volume flow Q and as $I=F(Q,T)$, where input water temperature T is a parameter [79].

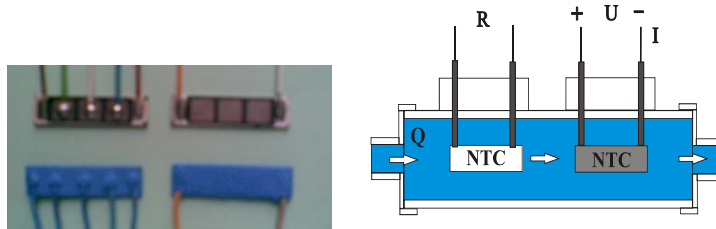


Fig. 11 Flowmeter for water based on heat loss of segmented thermistors: segmented thermistors with reduced dimensions (left) and cross section of flowmeter (right): cold thermistor (R) – serves as thermometer for measuring input water temperature T, and selfheated thermistor at constant voltage U and selfheating current I measures volume water flow Q.

The response of flowmeter on current water flow Q is given in figure 12: left diagram represents response of ultrasonic flowmeter as referent and right diagram represents thermal flowmeter for water with segmented thermistors. Two impulses were generated $Q=0.15$ [l/s] duration 30 s, 30 s pause and $Q=0.15$ [l/s] duration 30 s by fast switching of water flow using valves with lever.

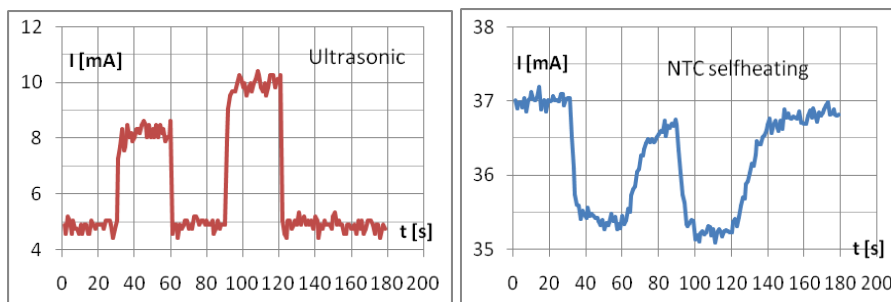


Fig. 12 The electrical response of thermal flowmeter on current volume water flow: impulse water function input $Q = 0.15$ l/s and $Q = 0.2$ l/s time duration 15s . Left diagram measured on referent ultrasonic flowmeter, right diagram measured on thermal flowmeter comprising segmented thermistor with reduced dimensions.

Their responses are given as electrical current I of ultrasonic flowmeter (output amplifier) and selfheating current I of NTC segmented thermistor, respectively. Input water temperature is $T=14.35$ °C, thermistor supply voltage $U=14.7$ V. The beginning and stop of water flow is detected by gradient of voltage measured on inner electrodes of thermistor. Moreover, thick film segmented thermistors also can be applied as gradient

sensors for measuring heat transfer from air to ground. Other possible applications of thick film thermistor are thick film thermistor bridges, hybrid circuits with thermistors, bolometers for radiation heat measuring and thermistor arrays for measuring heat transfer and temperature or heat homogeneity etc.

5. DISCUSSION AND CONCLUSION

Metal oxide thermistors have higher sensitivity comparing to other temperature dependent devices (table 1), higher accuracy and stability, lower response time and lower size, and lower price /performance. Therefore they are more suitable for application in different types of electronics: both PTC and NTC thermistors are widely produced as disc and chip shaped electrical components for many years, but NTC thermistors are more applied in temperature measurements as they have moderate exponential behavior with temperature (figure 1). NTC thermistors cover wide operation temperature range from -100 to 1200 °C using different metal oxides (table 2).

Thick film thermistors with rectangular geometry (or flip chip) have appeared recently as SMD (surface mounting device) commercial electrical component (Tateyama Kagaku Device Technology Co., Ltd.). The main advantage of thick film chip thermistors is in laser trimming of resistance and in faster response to temperature change due to thermal conductivity of alumina used as a substrate for thick film thermistor layer. Another advantage of thick film thermistors is in their sensitivity, due to thermistor layer low thickness (in microns), and low heat power for resistance change (a few mW). Thick film thermistors are designed for application in microelectronics e.g. for temperature compensation of other devices and temperature sensing. Their delay is as low as few seconds (transition from initial linear to non-linear regime), while sintered disc and chip thermistors are bulky and have much longer delay time.

Nickel manganese and other NTC thermistors which operate near room temperatures (low temperature range) are often in use in electronics as leaded or leadless electrical components for temperature measurements. Thick film thermistors are used much less as hybrid components: they are used mainly as custom designed hybrid planar components for thermal sensors. High temperature operating thick film thermistors are very rarely used for sensors applications above 300-400 °C. In practice thick film thermistor pastes appear as sensor pastes or as resistive pastes: they are produced for low temperature range applications (-50 to 130° C), with nominal square resistances 1, 10 or 100 [KΩ/□] at room temperature (ESL, Koartan, Heraeus). The modified nickel manganese thermistor pastes developed recently and presented in this work also belong to custom design sensor pastes, which are aimed for temperature sensors: they have mesoporous structure and moderate NTC slope (see figure 2 and 3), and enable realization round 10 times lower resistance than pure nickel manganite thermistor paste (see table 3).

Different thick film thermistor devices (planar geometries) were analyzed and optimized to achieve suitable resistance and power dissipation of thick film thermistors and achieve faster response of thermistors needed for heat loss sensors. Optimization of resistance included influence of electrode shape, size and arrangement, electrode spacing and diffusion of metal electrode to thermistor layer or electrode effect to sheet resistance (figure 5 and 6). Mutual comparison of thick film thermistor geometries shows that sandwich

and multilayer geometries are “low ohmic” while rectangular and interdigitated geometries are “high ohmic” (Ω and $M\Omega$, respectively). A new geometry called segmented thermistor appeared as “moderate ohmic” geometry ($k\Omega$), and most suitable for heat loss sensor. Segmented thermistors were designed, realized and applied for heat loss from 1-5 W (different size and number of segments as given in figure 8). The equations (1) and (2), given above in part 5, are basic for resistance calculations, modeling and designing, and simulation e.g. predicting of properties of created new geometries, before thick film thermistor printing, sintering and measuring.

The three axes anemometers and water flow sensors (presented above) are fully thermal devices based on selfheated thick film thermistors and heat loss principle. Comparing to electromechanical or ultrasonic flowmeters they are simpler: they do not contain amplifiers or moving parts, they are smaller in size and cheaper. The aim was to develop intelligent sensors as the second step of research and introduce intelligent functions such as auto-range, auto-calibration, auto-correction of delay and auto-display of measured values and calculated values, selection of continual or switching operating mode, etc.

Finally, summing the recent advances in thick film thermistors three tendencies can be noticed: 1. New thermistor materials development, 2. New custom designed thermistor pastes development (micro/nano structured and doped with different oxides including rare earths) and 3. New thick film geometries development (planar constructions) aimed for thermistor sensors and systems. All three tendencies combined lead to novel thick film thermistors e.g. to new applications which fit the customer requirements. The new applications such as thick film gradient temperature sensor, temperature sensor array, bolometer with high temperature thermistor are partly in realization and their appearance is expected very soon in near future.

Acknowledgement: *The paper is a part of the research done within the project III 45 007 financed by the Ministry of Education, Science and Technological Development of Serbia.*

REFERENCES

- [1] P. R. N. Childs, J. R. Greenwood, C. A. Long, “Review of temperature measurement”, *Review Scientific Instrumentation*, vol. 71, no. 8, pp. 2959-2965, 2000.
- [2] T. D. Mc Gee, *Principles and Methods of Temperature Measurement*, John Wiley, 1988, pp. 2-21
- [3] N.G. Lewis, M. Randall, *Thermodynamics*, 2nd edition, McGraw-Hill, New York, 1961, pp. 378-379.
- [4] D. Sherry, “Thermoscopes, thermometers, and the foundations of measurement”, *Studies in History and Philosophy of Science*, vol. 42, pp. 509–524, 2011.
- [5] P. Coates, D. Lowe, *The Fundamentals of Radiation Thermometers*, Chapter 1: The Basis of Temperature Measurement, CRC Press 2016, pp. 10-30.
- [6] M. J. Moran, H. N. Shapiro, *Fundamentals of Engineering Thermodynamics*, Chapter 1, John Wiley & Sons, 2006, pp. 10-25.
- [7] J. G. Webster, H. Eren, *Measurement, Instrumentation and Sensor Handbook*, Thermal and temperature measurement, Chapter 7, 2nd edition, CRC Press 2014, pp. 65-78.
- [8] B. L. Hunt, “The early history of the thermocouple”, *Platinum Metals Rev.*, vol. 8, no. 1, pp. 23-28, 1964.
- [9] Y.S. Touloukian, D.P. DeWitt P.D., *Thermophysical Properties of Matter*, TPRC Series, vol. 7 - Thermal Radiative Properties, Metallic Element and Alloys, IFI/Plenum NY, 1970, pp. 159-168.
- [10] R.E. Bentley, *Handbook of temperature measurement*, vol. 3: Theory and practice of thermoelectric thermometry. Springer-Verlag Singapore Pte. Ltd., 1998, pp. 24-36.

- [11] R.A. Felice, "Pyrometry for liquid metals", *Advanced Materials & Processes*, vol.166 (7), ASM International, pp. 31-33, 2008.
- [12] R. P. Benedict, *Fundamentals of Temperature, Pressure, and Flow Measurements*, Third Edition, Chapter 8. Optical Pyrometry, John Wiley 1984, pp. 130-145.
- [13] E.D. Macklean, *Thermistors*, Electrochem. Pub., Glasgow, 1979, pp. 5-22.
- [14] F. J. Hyde, *Thermistors*, First Edition, Published by ILIFFE, 1971, pp. 2-15.
- [15] D. R. White, "Temperature errors in linearizing resistance networks for thermistors", *International Journal of Thermophysics*, vol. 36, no. 12, pp. 3404–3420, 2015.
- [16] P. Umadevi, C. L. Nagendra, "Preparation and characterization of transition metal oxide micro-thermistors and their application to immersed thermistor bolometer infrared detectors", *Sensors and Actuators A: Physical*, vol. 96, no. 2–3, pp. 114-124, 2002.
- [17] H. Zumbahlen, *Linear Circuits Design Handbook*, Chapter 3-2 Temperature sensors: Thermistors, Analog Devices -Newnes, 2008, pp. 231-240.
- [18] W. Kester, J. Bryant, W. Jung, *Sensor Signal Conditioning, Temperature Sensors*, Chapter 7, Analog Devices, pp. 1-38, 2000.
- [19] D. D. Pollock, *Thermocouples: theory and properties*, CRC Press, 1991, pp. 181- 195.
- [20] B. Gosselin Jr, "NTC thermistors versus voltage output IC temperature sensors", *Texas Instruments ECN*: 04/02/2013, pp. 1-3.
- [21] T. Kuglestadt, "Semiconductor Temperature Sensors Challenge Precision RTDs and Thermistors in Building Automation", *Texas Instruments: Application Report*: SNAA267–04 2015, pp. 2-10.
- [22] T.G. Nanov, S.P. Yordanov, *Ceramic Sensors: Technology and Applications*, Chapter 5 Thermistors, CRC Press, 1996, pp. 193-203.
- [23] C. Ma, Y. Liu, Y. Lu, H. Qian, "Preparation and electrical properties of Ni_{0.6}Mn_{2.4x}Ti_xO₄ NTC ceramics", *Journal of Alloys and Compounds*, vol. 650, pp. 931-935, 2015.
- [24] J. Park, "Microstructural and electrical properties of Y_{0.2}Al_{0.1}Mn_{0.27-x}Fe_{0.16}Ni_{0.27-x}(Cr_{2x})O_y for NTC thermistors", *Ceramics International*, vol. 41, no. 5, pp. 6386-6390, 2015.
- [25] O. Shpotyuk, A. Kovalskiy, O. Mrooz, L. Shpotyuk, V. Pechnyo, S. Volkov, "Technological modification of spinel-based Cu_xNi_{1-x-y}Co_{2y}Mn_{2-y}O₄ ceramics", *Journal of the European Ceramic Society*, vol. 21, no. 11-12, pp. 2067–2070, 2001.
- [26] R. Metz, "Electrical properties of N.T.C. thermistors made of manganite ceramics of general spinel structure: Mn_{3-x-x'}M_xN_xO₄ (0 ≤ x + x' ≤ 1; M and N being Ni, Co or Cu). Aging phenomenon study", *Journal of Materials Science*, vol. 35, pp. 4705–4711, 2000.
- [27] R.C. Buchanan, *Ceramic Materials for Electronics: Processing, Properties and Applications* (Electrical Engineering & Electronics), Marcel Dekker Inc; Enlarged 2nd edition, 1986, pp. 125-162.
- [28] M. Vakiv, O. Shpotyuk, O. Mrooz, I. Hadzaman, "Controlled thermistor effect in the system Cu_xNi_{1-x-y}Co_{2y}Mn_{2-y}O₄", *Journal of the European Ceramic Society*, vol. 21, pp. 1783–1785, 2001.
- [29] E. S. Na, U. G. Paik, S. C. Choi, "The effect of a sintered microstructure on the electrical properties of a Mn-Co-Ni-O thermistor", *Journal of Ceramic Processing Research*, vol. 2 (1), pp. 31- 34, 2001.
- [30] H. Zhang, A. Chang, C. Peng, "Preparation and characterization of Fe³⁺-doped Ni_{0.9}Co_{0.8}Mn_{1.3-x}Fe_xO₄ (0 < x < 0.7) negative temperature coefficient ceramic materials", *Microelectronic Engineering*, vol. 88, no. 9, pp. 2934–2940, 2011.
- [31] M. L. M. Sarrión, M. M. Sánchez, "Preparation and characterization of thermistors with negative temperature coefficient, Ni_xMn_{3-x}O₄ (1 < x < 0.56), from formate precursors", *J. Mater. Chemistry*, vol. 3, pp. 273-277, 1993.
- [32] C. Ma, Y. Liu, Y. Lu, H. Gao, H. Qian, J. Ding, "Preparation and characterization of Ni_{0.6}Mn_{2.4}O₄ NTC ceramics by solid-state coordination reaction", *J Materials Science: Materials in Electronics*, vol. 24, no. 12, pp. 5183–5188, 2013.
- [33] D. Fang, C. G. Lee, B. H. Koo, "Preparation of Ultra-Fine FeNiMnO₄ Powders and Ceramics by a Solid-State Coordination Reaction", *Metals and Materials International*, vol. 13, no. 2, pp. 165-170, 2007.
- [34] K. Park, I.H. Han, "Effect of Al₂O₃ addition on the microstructure and electrical properties of Mn_{0.37}Ni_{0.3}(Co_{0.33-x}Al_x)O₄ (0 ≤ x ≤ 0.03) NTC thermistors", *Materials Science and Engineering, B* vol. 119, pp. 55-60, 2005.
- [35] P. Ouyang, H. Zhang, Y. Zhang, J. Wang, Z. Li, "Zr substituted SnO₂-based NTC thermistors with wide applications temperature range and high property stability", *Journal of Materials Science: Materials in Electronics*, vol. 26, no. 8, pp. 6163–6169, 2015.
- [36] R. K. Kamat, G. M. Naik, "Thermistors – in search of new applications, manufacturers cultivate advanced NTC techniques", *Sensor Review*, vol. 22, no. 4, pp. 334 - 340, 2002.
- [37] T. Yang, B. Zhang, Q. Zhao, P. Luo, A. Chang, "New high temperature NTC thermistors based on the Mg(Al_{1-x}Cr_x)₂O₄ ceramics", *Journal of Alloys and Compounds*, vol. 685, pp. 287–293, 2016.

- [38] W. Lee and J. Park, "NTC Thermistors of Y-Al-Mn-Fe-Ni-Cr-O Ceramics for Wide Temperature Range Measurement", In Proceedings of the 8th International Conference on Sensing Technology, Sep. 2-4, 2014, Liverpool, pp. 307-310.
- [39] B. Zhang, Q. Zhao, A. Chang, H. Yan, Y. Wu, "MgAl₂O₄-LaCr_{0.5}Mn_{0.5}O₃ composite ceramics for high temperature NTC thermistors", *J Mater Science: Materials in Electronics*, vol. 24, no. 11, pp. 4452-4456, 2013.
- [40] S. Subhanarayan, S. K. S. Parashar, S. M. Ali, "CaTiO₃ nano ceramic for NTCR thermistor based sensor application", *Journal of Advanced Ceramics*, vol. 3, no. 2, pp. 117-124, 2014.
- [41] A. Feltz, R. Krigel, W. Polzl, "Sr₇Mn₄O₁₅ ceramics for high temperature NTC thermistors", *Journal of Material Science Letters*, vol. 18, no. 20, pp. 1693-1695, 1999.
- [42] K. Park, "Microstructure and electrical properties of Ni_{1.0}Mn_{2-x}Zr_xO₄ (0 ≤ x ≤ 1.0) negative temperature coefficient thermistors", *Materials Science and Engineering, B* vol. 104, no. 1-2, pp. 9-14, 2003.
- [43] W. Wasluluddin, D. G. Syarif, "Effect of MnO₂ Addition on Characteristics of Fe₂TiO₅ Ceramics for NTC Thermistor Utilizing Commercial and Local Iron Oxide", *Journal of The Australian Ceramic Society*, vol. 49, no. 2, pp. 141-147, 2013.
- [44] Y. Luo, X. Liu, "High temperature NTC BaTiO₃-based ceramic resistors", *Materials Letters*, vol. 59, no. 29-3, pp. 3881 - 3884, 2005.
- [45] W. Lee and J. Park, "NTC Thermistors of Y-Al-Mn-Fe-Ni-Cr-O Ceramics for Wide Temperature Range Measurement", In Proceedings of the 8th International Conference on Sensing Technology, Sep. 2-4, 2014, Liverpool, UK, pp. 307-310.
- [46] C. Yuan, X. Liu, M. Liang, C. Zhou, H. Wang, "Electrical properties of Sr-Bi-Mn-Fe-O thick-film NTC thermistors prepared by screen printing", *Sensors and Actuators*, vol. A 167, pp. 291-296, 2011.
- [47] R. Schmidt, A.W. Brinkman, "Electrical properties of screen-printed NiMn₂O_{4+δ}", *Journal of the European Ceramic Society*, vol. 25, no. 12, pp. 3027-3031, 2005.
- [48] X. Xiong, J. Xu, P. Zhao, L. Wang, L. Bian, F. Xu, J. Zhang, A. Chang, "Structural and electrical properties of thick film thermistors based on perovskite La-Mn-Al-O", *Ceramics International*, Part B, vol. 40, no. 7, pp. 10505-10510, 2014.
- [49] Y. Yang, C. Yuan, G. Chen, T. Yang, Y. Luo, C. Zhou, "Effect of Ba_{0.5}Bi_{0.5}Fe_{0.9}Sn_{0.1}O₃ addition on electrical properties of thick-film thermistors", *Transactions of Nonferrous Metals Society of China*, vol. 25, no. 12, pp. 4008-4017, 2015.
- [50] C.L. Yuan, X.Y. Liu, C.R. Zhou, J.W. Xu, B. Li, "Electrical properties of lead-free thick film NTC thermistors based on perovskite-type BaCo^{II}_xCo^{III}_{2-x}Bi_{1-3x}O₃", *Materials Letters*, vol. 65, no. 5, pp. 836-839, 2011.
- [51] C. Yuan, X. Wu, J. Huang, X. Liu, B. Li, "Electrical properties of thick film NTC thermistors based on SrFe_{0.9}Sn_{0.1}O_{3-δ}", *Solid State Sciences*, vol. 12, no. 12, pp. 2113-2119, 2010.
- [52] S. Jagtap, S. Rane, S. Gosavi, D. Amalnerkar, "Low temperature synthesis and characterization of NTC powder and its 'lead free' thick film thermistors", *Microelectronic Engineering*, vol. 87, no. 2, pp.104-107, 2010.
- [53] S. Jagtap, S. Rane, S. Gosavi, D. Amalnerkar, "Preparation, characterization and electrical properties of spinel-type environment friendly thick film NTC thermistors", *Journal of the European Ceramic Society*, vol. 28, no. 13, pp. 2501-2507, 2008.
- [54] K. Park, "Structural and electrical properties of FeMg_{0.7}Cr_{0.6}Co_{0.7-x}Al_xO₄ (0≤x≤0.3) thick film NTC thermistors", *Journal of the European Ceramic Society*, vol. 26, no. 6, pp. 909-914, 2006.
- [55] K. Park, D.Y. Bang, "Electrical properties of NiMn-Co(Fe) oxide thick film NTC thermistors", *Journal of Materials Science: Materials in Electronics*, vol. 14, pp. 81-87, 2003.
- [56] O.S. Aleksić, P.M. Nikolić, D.G. Vasiljević-Radović, M.D. Luković, S.Djurić, M.N. Simić, V.Ž. Pejović, K.T. Radulović, D. Vujošević, D. Luković, "Properties of Thick Film NTC Layers Based on Nanometric Mn,Co,Fe-Oxide Powder Mixture", Printed in book *Science of sintering: Current problems and New Trends*, editor M.M.Ristić, SANU press, 2003, pp. 427-32.
- [57] S. Savic, O. S. Aleksic, P. M. Nikolic, D. T. Lukovic, "Geometrical and electrical properties of NTC polycrystalline thermistors vs. changes of sintering parameters", *Science of Sintering*, vol. 38, no. 3, pp. 223-229, 2006.
- [58] M. V. Nikolic, K. M. Paraskevopoulos, O. S. Aleksic, T. T. Zorba, S. M. Savic, V. D. Blagojevic, D. T. Lukovic, P. M. Nikolic, "Far infrared reflectance of sintered nickel-manganite samples used as negative temperature coefficient thermistors", *Materials Research Bulletin*, vol. 42, pp. 1492-1498, 2007.
- [59] S. M. Savic, G. M. Stojanovic, M. V. Nikolic, O. S. Aleksic, D. T. Lukovic-Golic, P. M. Nikolic, "Electrical and transport properties of nickel manganite obtained by Hall effect measurements", *Journal of Materials Science: Materials in Electronics*, vol. 20, no. 3, pp. 242-247, 2009.

- [60] S. M. Savic, M. V. Nikolic, O. S. Aleksic, M. Slankamenac, M. Zivanov, P. M. Nikolic, "Intrinsic resistivity of sintered nickel manganite vs. powder activation time and density", *Science of Sintering*, vol. 40, no. 1, pp. 27-32, 2008.
- [61] O.S. Aleksic, P.M. Nikolic, D. Lukovic, K. Radulovic, D. Vasiljevic-Radovic, P. Nikolidis, "Investigation of the thermal diffusivity for thick film NTC layers by photoacoustic technique", *Microelectronics International*, vol. 21, no. 1, pp. 10-14, 2004.
- [62] O. S. Aleksic, P. M. Nikolic, D. Lukovic, S. Savic, D. Vasiljevic-Radovic, K. Radulovic, L. Lukic, A. Bojicic, D. Urosevic, "Investigation of the thermal diffusivity of thick film NTC layers obtained with the photoacoustic method", *Journal de Physique IV, France*, vol. 125, pp. 431-433, June 2005.
- [63] S. M. Savić, O. S. Aleksić, M. V. Nikolić, D. T. Luković, V. Ž. Pejović, P. M. Nikolić, "Thermal diffusivity and electron transport properties of NTC samples obtained by photoacoustic method", *Materials Science and Engineering B*, vol. 131, no. 1-3, pp. 216-221, 2006.
- [64] O. S. Aleksic, M. V. Nikolic, M. D. Lukovic, N. Nikolic, B. Radojicic, M. Radovanovic, Z. Z. Djuric, M. Mitric, P. M. Nikolic, "Preparation and characterization of Cu and Zn modified nickel manganite NTC powders and thick film thermistors", *Mater Sci. Eng. B*, vol. 178, no. 3, pp. 202-210, 2013.
- [65] O.S. Aleksic, P.M. Nikolic, D.M. Todorovic, "Analysis and Synthesis of Thick Film Resistor Using EGET Principles", *Hybrid Circuits, (Microelectronics International)*, vol. 5, no. 3, pp. 20-23, 1988.
- [66] O. S. Aleksic, B. M. Radojicic, R. M. Ramovic, "Modeling and simulation of NTC thick film thermistor geometries", *Microelectronics International*, vol. 24, no. 1, pp. 27-34, 2007.
- [67] O. S. Aleksic, V. Dj. Maric, Lj. D. Zivanov, A. B. Menicanin, "A novel approach to modeling and simulation of NTC thick-film segmented thermistors for sensor applications", *IEEE Sensors Journal*, vol. 7, no. 10, pp. 1420-1428, 2007.
- [68] V. Dj. Maric, M. D. Lukovic, Lj. D. Zivanov, O. S. Aleksic, A. B. Menicanin, "EM simulation analysis of optimal performance thick film segmented thermistors versus materials characteristics selection", *IEEE Transactions on Instrumentation and Measurement*, vol. 57, no. 11, pp. 2568-2575, 2008.
- [69] J. S. Steinhart, S.R. Hart, "Calibration curves for thermistors", *Deep-Sea Research and Oceanographic Abstracts*, vol.15, no. 4, pp. 497-503, 1968.
- [70] S. Rudtsch, C. von Rohden, "Calibration and self-validation of thermistors for high-precision temperature measurements", *Measurement*, vol. 76, pp. 1-6, December 2015.
- [71] C. Chen, "Evaluation of resistance-temperature calibration equations for NTC thermistors", *Measurement*, vol. 42, no. 7, pp. 1103-1111, 2009.
- [72] S.B. Stanković, P.A. Kyriacou, "The effects of thermistor linearization techniques on the T-history characterization of phase change materials", *Applied Thermal Engineering*, vol. 44, no. 11, pp. 78-84, 2012.
- [73] O.S. Aleksic, "Three dimensional anemometer comprising thick film segmented thermistors", (WO-2007-014400), Published in Patent Gazette, International Bureau WIPO, Geneve, Swiss, 1.02.2007, <http://patentscope.wipo.int/search>, Google type: WO-2007-014400, pp. 1-18.
- [74] A.B Menicanin, O.S Aleksic, M.V Nikolic, S.M Savic, B.M Radojicic, "Novel uniaxial anemometer containing NTC thick film segmented thermistors", Proceedings of the 26th International Conference of Microelectronics 11-14 May 2008 (IEEE MIEL), pp. 349-352.
- [75] O. S. Aleksic, S. M. Savic, M. D. Lukovic, K. T. Radulovic, L. S. Lukic, "Segmented thermistors printed by NTC nanometric paste and applied in volume air-flow sensors", *Materials Science Forum: Recent Developments in Advanced Materials and Processes*, vol. 518, pp. 247-252, 2006.
- [76] O. S. Aleksic, P. M. Nikolic, K. M. Paraskevopoulos, "Volume air flow sensors based on NTC thick film segmented thermistors", *Microelectronics International*, vol. 23, no. 3, pp. 14-18, 2006.
- [77] O. S. Aleksic, S. M. Savic, M. V. Nikolic, L. Sibinoski, M. D. Lukovic, "Micro flow sensor for water using NTC thick film segmented thermistors", *Microelectronics International*, vol. 26, no. 3, pp. 30-34, 2009.
- [78] M. V. Nikolic, B. M. Radojicic, O. S. Aleksic, M. D. Lukovic, P. M. Nikolic, "A thermal sensor for water using self-heated NTC thick-film segmented thermistors", *IEEE Sensors Journal*, vol. 11, no. 8, pp.1640-1645, 2011.
- [79] O. S. Aleksic, M. V. Nikolic, M. D. Lukovic, Z. I. Stanimirovic, I. P. Stanimirovic, L. Z. Sibinoski, "The response of a heat loss flowmeter in a water pipe under changing flow conditions", *IEEE Sensors Journal*, vol. 16, no. 9, pp. 2935-2941, 2016.